Free Space Transmission Measurements of Ultra Wideband Antenna for Wireless Personal Area Networks

Sathaporn Promwong[†§], Wataru Hanitachi[§], Jun-ichi Takada[§], Pichaya Supanakoon[†], Monchai Chamchoy[†], Prakit Tangtisanon[†], and Vech Vivek[‡]

[§]Graduate School of Science and Engineering,
Tokyo Institute of Technology
2-12-1, O-okayama, Meguro-ku, Tokyo 152-8552, Japan.
E-mail: {ken,takada}@ap.ide.titech.ac.jp

[†]Department of Information Engineering, Faculty of Engineering,
King Mongkut's Institute of Technology Ladkrabang, Bangkok 10520, Thailand.
E-mail: {kspichay,kcmoncha, ktprakit}@kmitl.ac.th

[‡]Department of Electrical Engineering, Faculty of Engineering,
King Mongkut's Institute of Technology North Bangkok, Bangkok 10800, Thailand
E-mail: vvv@kmitnb.ac.th

Abstract

This paper reports a free space transmission measurements of ultra wideband antenna for wireless personal area networks. The measurement system consists of transmitted and received biconical antennas measured by a vector network analyzer. To obtain the data, measurements were performed at 3 GHz to 11 GHz covered by a vector network analyzer, which provided information on the amplitude and phase of the transmission coefficient. Friis' transmission formula is not directly applicable and the wavefrom distortion may degrade the transmission performance as well. The matched filter reception is considered to maximize the SNR at the receiver for the evaluation. Some experimental examples are shown.

Keywords: Ultra Wideband (UWB), Ultra Wideband Antenna, UWB Measurements, Friis' transmission formula.

1. Introduction

Ultra wideband (UWB) radio technology has become one important topic for wireless communication. The UWB radio communications can be viewed as an extreme form of spread spectrum communication system. UWB radios are generally defined to have a 3 dB bandwidth which is greater than 25 % of the center frequency or greater than 1.5 GHz. A bandwidth for UWB radio signals can be defined by the fraction bandwidth B_f as [1], [2]

$$B_f = 2\frac{f_H - f_L}{f_H + f_L}, \tag{1}$$

where f_H and f_L are the highest and lowest frequency of the signal spectrum, respectively. This large bandwidth can be achieved by driving an appropriately designed antenna with very short electrical pulses. Due to the 'carrier-less' characteristics where no sinusoidal carrier raises the signal to a certain frequency band, the UWB systems are also referred as base band communication systems. Typically, the radiated pulse signals are generated without the use of local oscillators or mixers, thus results in a simpler and cheaper construction of transmitter (Tx) and receiver (Rx). The electromagnetic pulses with the duration of the order of a few nanoseconds to a fraction of nanoseconds were generated and radiated. The large transmission bandwidth, from near d.c. to a few GHz, has resulted in higher immunity to interference effects and improved multipath fading robustness. The UWB technology is an ideal candidate that can be utilized for commercial, short-range, low power, low cost indoor communication systems such as Wireless Personal Area Network (WPAN) [3]-[5].

The United States Federal Communications Commission (FCC) is currently working on setting emission limits that would allow UWB communication systems to be deployed on an unlicensed basic following the Part 15 rules for radiated emissions of intentional radiators [6]. The UWB radio channel bandwidth for handheld wireless communications is from 3.1 GHz to 10.6 GHz. The power spectrum density level of UWB signal may be below the noise level of the receivers for other systems. The UWB receiver collects the power of received signal for rebuilding the pulse. Therefore, the UWB radio technology can exist with other RF technologies without the interference.

In UWB communication, the antennas are significantly pulse-shaping filters. Any distortion of the signal in the frequency domain causes the distortion of the transmitted pulse shape. Consequently, this will increase the complexity of the detection mechanism at the receiver [7]. The antenna design for UWB signal radiation is one of the main challenges [8]-[10]. Especially, low cost, geometrically small and still efficient structures are required for typical wireless applications such as WPAN.

In this paper, we discuss the free space transmission measurements of UWB antenna. This technique is based on the Friis' transmission formula, in the sense that we would like to derive the equivalent antenna gain for UWB systems. The transmission waveform and the matched filter reception are keys for the extension of the Friis' formula to UWB. We carried out an experiment using the biconical antenna for UWB operation on the flat top of the roof.

2. Extension of Friis' Transmission Formula for UWB Systems

In this study, we focus on the link budget evaluation in the free space. For the narrowband systems, Friis' transmission formula [11] have been widely used.

$$G_{\mathrm{Friis}} = \frac{P_{\mathrm{r}}}{P_{\mathrm{t}}} = G_{\mathrm{f}} G_{\mathrm{r}} G_{\mathrm{t}}, \tag{2}$$

where G_{r} and G_{t} are Rx and Tx antenna gain,

$$G_{\mathrm{f}} = \left(\frac{\lambda}{4\pi d}\right)^2, \tag{3}$$

is the free space propagation gain (less than unity in practice), $\lambda = c/f$ is the wavelength, c is the velocity of the light, and f is the frequency.

It is noted, however, that Eq. (2) is satisfied only at some certain frequency, and is not directly applicable to UWB systems. We have recently proposed a new extension of the Friis' transmission formula to take into account the transmission signal waveform and its distortion as well [12]. The results are summarized as follows. The detailed derivation is presented in [12].

Input signal $v_{\mathrm{i}}(t)$ at the transmitter port is expressed as the convolution of an impulse and the pulse shaping filter as

$$v_{\mathrm{i}}(t) = E_{\mathrm{i}} \delta(t) * h_{\mathrm{i}}(t), \tag{4}$$

where

$$\int_{-\infty}^{\infty} h_{\mathrm{i}}^2(t)\mathrm{d}t = \int_{-\infty}^{\infty} |H_{\mathrm{i}}(f)|^2 \,\mathrm{d}f = 1. \tag{5}$$

Friis' formula is extended taking into account the transmission waveform as

$$H_{\mathrm{e-Friis}}(f) = \frac{V_{\mathrm{r}}(f)}{E_{\mathrm{i}}} = H_{\mathrm{f}} H_{\mathrm{i}} \mathbf{H}_{\mathrm{r}} \cdot \mathbf{H}_{\mathrm{t}}, \tag{6}$$

where

$$\begin{aligned} \mathbf{H}_a &= \mathbf{H}_a(\theta_a, \varphi_a, f), \\ &= \hat{\theta}_a \mathbf{H}_{a\theta}(\theta_a, \varphi_a, f) + \hat{\varphi}_a \mathbf{H}_{a\varphi}(\theta_a, \varphi_a, f), \\ a &= \mathrm{r} \ \mathit{or}\ \mathrm{t}, \end{aligned} \tag{7}$$

is a complex transfer function vector of the antenna relative to the isotropic antenna,

$$H_{\mathrm{f}} = \frac{\lambda}{4\pi d} \exp(-\jmath k d), \tag{8}$$

is the free space transfer function where

$$k = \frac{2\pi}{\lambda}, \tag{9}$$

is the propagation constant. Unit vectors $\hat{\theta}_a$, $\hat{\varphi}_a$ to express the polarization are defined with respect to the local polar coordinates of the each of the antennas. The following relations can be easily derived

$$\hat{\theta}_{\mathrm{r}} = \hat{\theta}_{\mathrm{t}}, \tag{10}$$

$$\hat{\varphi}_{\mathrm{r}} = -\hat{\varphi}_{\mathrm{t}}. \tag{11}$$

At the receiver, the matched filter $H_{\mathrm{MF(f)}}$ is introduced to maximize the signal-to-noise ratio (SNR) of the receiver output, as shown in Fig. 1.

$$H_{\mathrm{MF}}(f) = \frac{H^*_{\mathrm{e-Friis}}(f)}{\sqrt{\int_{-\infty}^{\infty} |H_{\mathrm{e-Friis}}(f)|^2 \,\mathrm{d}f}}, \tag{12}$$

which satisfies the following constant noise output power condition

$$\int_{-\infty}^{\infty} |H_{\mathrm{MF}}(f)|^2 \,\mathrm{d}f = 1. \tag{13}$$

In case, the output waveform when $E_{\mathrm{i}} = 1$

$$v_{\mathrm{MF}}(t) = h_{\mathrm{e-Friis}}(t) * h_{\mathrm{MF}}(t), \tag{14}$$

takes its maximum at $t = 0$ as

$$\begin{aligned} \max_t v_{\mathrm{MF}}(t) = v_{\mathrm{MF}}(0) &= \int_{-\infty}^{\infty} V_{\mathrm{MF}}(f)\mathrm{d}f, \\ &= \sqrt{\int_{-\infty}^{\infty} |H_{\mathrm{e-Friis}}(f)|^2 \,\mathrm{d}f}. \end{aligned} \tag{15}$$

Equation (15) is the UWB extension of Friis' transmission formula. This equation includes three elements, i.e., the frequency characteristics of the antennas, the frequency characteristics of free space propagation, and the spectrum of the transmit signal.

3. Preparation for the Experiments

In this section, some issues of the preparation for the experiments are described [13].

3.1 UWB Signal Model

The effect of the waveform distortion is more obvious when the bandwidth is wider. We considered the impulse radio signal that fully covers the FCC band [6], i.e., 3.1∼10.6 GHz. The center frequency and the bandwidth were therefore set to be $f_0 = 6.85$ GHz and $f_{\mathrm{b}} = 7.5$ GHz, respectively. The transmit waveform assumed in the simulation was a single ASK pulse with the carrier frequency f_0. To satisfy the bandwidth requirement of f_{b}, the pulse

CM05

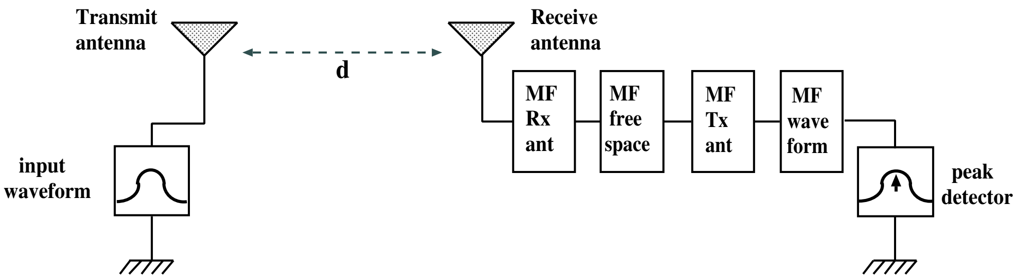

Fig. 1. Block diagram of transmission system for the extension of Friis' transmission formula to treat UWB signal.

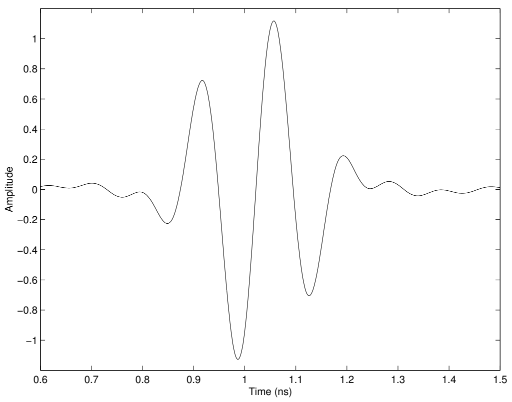

Fig. 2. The transmission waveform of UWB signal.

length was set to be $2/f_b$. Then the signal was band-limited by the Nyquist roll-off filter with the roll-off factor $\alpha = 0$ (rectangular window) and the passband $(f_0 - f_b/2,\ f_0 + f_b/2)$. Figure 2 shows the transmit pulse waveform.

All the transmission simulations of the pulse waveforms are simulated based on the measured transfer functions of antennas.

3.2 Experiments Setup

An UWB radio channel transfer function was measured as S_{21} in frequency domain by using a vector network analyzer (VNA). The VNA was operated in the response measurement mode, where Port-1 was the transmitter port (Tx) and Port-2 was the receiver port (Rx), respectively. The measurement was done on the flat top of the roof of Tokyo Tech building. Both Tx and Rx antennas were fixed at the height of 1.3 m and were separated at 1 m. In this study, we considered a broadband antenna that was suitable for the operation with pulsed waveforms [14]. We have chosen this biconical antenna for the ease of the fabrication, as well as it is often used as the standard antenna.

3.3 Parameters of Experiments

The important parameters for the experiments are listed in Table 1.

Table 1. Experimental setup parameters.

Parameter	Value
Frequency range	3~11 GHz
Number of frequency points	1601
Dynamic power range	80 dB
IF bandwidth	3 MHz
Antenna type	Biconical
Tx antenna height	1.3 m
Rx antenna height	1.3 m
Distance between Tx and Rx	1.0 m
Pointing angle	0°/ 30°/ 60°

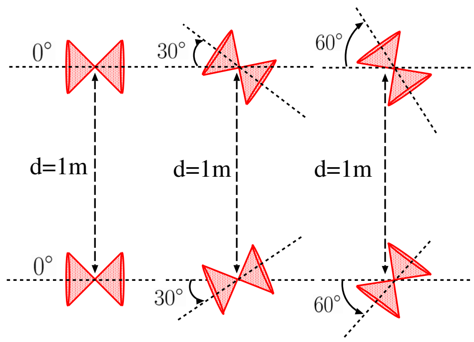

Fig. 3. Orientations of two biconical antennas.

It is noted that the calibration is done at the connectors of the cables to be connected to the antennas. Therefore, all the impairments of the antenna characteristics are included in the measured results. The orientations of the two biconical antennas are shown in Fig. 3.

4. Results of Experiments

Fig. 4 and Fig. 5 show the amplitude and the phase of the transfer function measured for three different antenna setups. From Fig. 4, the radiation pattern seems to change from frequency to frequency, which may result in the waveform distortion.

Fig. 6 shows the received pulse waveforms when the transmit waveform shown in Fig. 2 is input. For comparison, the waveform for isotropic antennas are

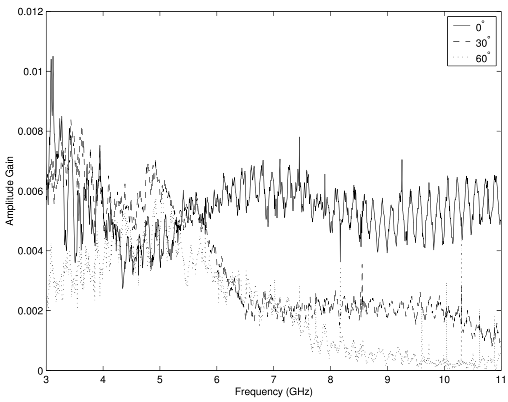

Fig. 4. Measured transfer functions for different antenna pointing conditions: amplitude.

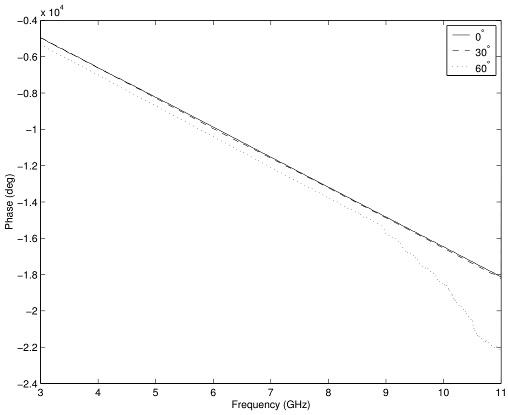

Fig. 5. Measured transfer functions for different antenna pointing conditions: phase.

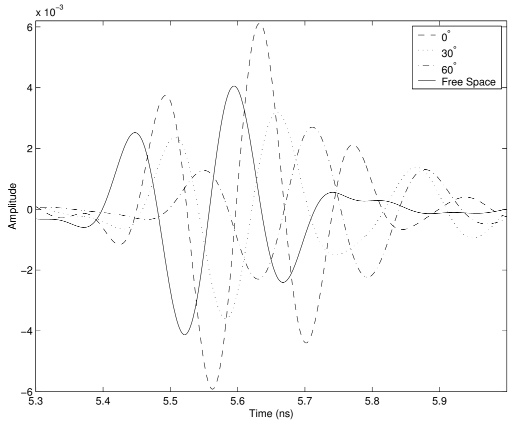

Fig. 6. Received waveform at the antenna output.

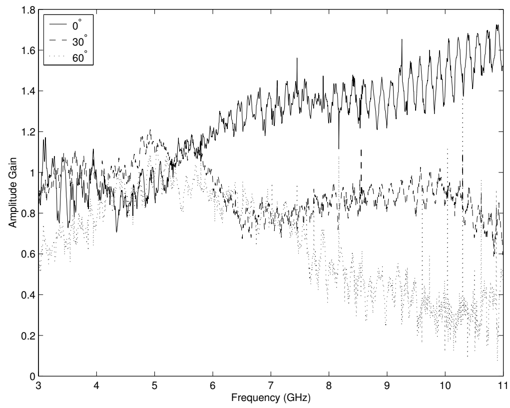

Fig. 7. Antenna transfer function: amplitude.

shown as "Free Space". Compared with the isotropic case, the pulse waveform is very much distorted and lengths become longer.

Although the accurate transfer function of each individual antenna shall be measured using three-antenna methods, Fig. 7 and Fig. 8 show the approximate antenna transfer function which are obtained by assuming that Tx and Rx antennas are identical. The vertical axis is normalized by the isotropic antenna. Therefore, for 0° and 30° positions, the directive gain is below 0 dB for almost frequency range.

Fig. 9 and Fig. 10 show the output of matched filters. In Fig. 9, the matched filter is optimized for the each individual scenario, and the results correspond to the maximum available gain. In contrast, for Fig. 10, the matched filter is replaced by that for isotropic antennas. This result is more realistic in practice, because the directions of the Tx and Rx antennas are not usually arbitrarily controllable, but set at the convenient positions.

Table 2 summarizes the overall gain with respect to the isotropic antennas case. Since the gain at the most of the frequencies was below unity, the dB value of the gain is negative. By using the approximate matched filter, the gain has been degraded.

As the amount of the gain degradation depends on the setups, Table 3 lists the correlation coefficient of the impulse responses between the received signal and the approximate matched filter using the isotropic antennas. For the case of 0°, the correlation coefficient is low compared with others. This is partly the reason why gain degradation by using the approximate matched filter is larger only for this case.

5. Conclusion

In this paper, we reported the experiment of the free space transmission characteristics of ultra wideband antenna. In the proposed scheme, Friis' transmission formula is extended in order to take into account the transmit waveform and the matched filter to the system. Experimental demonstration using the biconical antenna for UWB was shown, and the specific gain value could be obtained for Tx-Rx antenna pair.

In the present paper, we introduced the matched filter for the optimum receiver. However, if the distorted component should be regarded as the interference, the equalizer instead of the matched filter

CM05

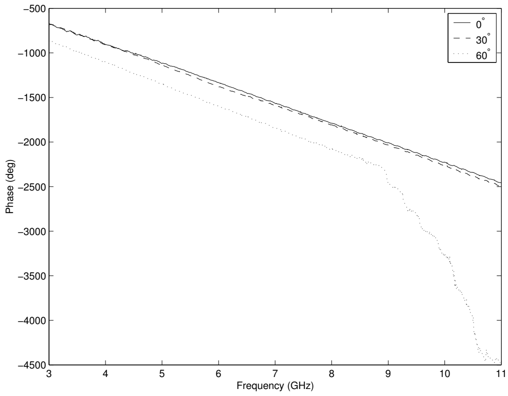

Fig. 8. Antenna transfer function: phase.

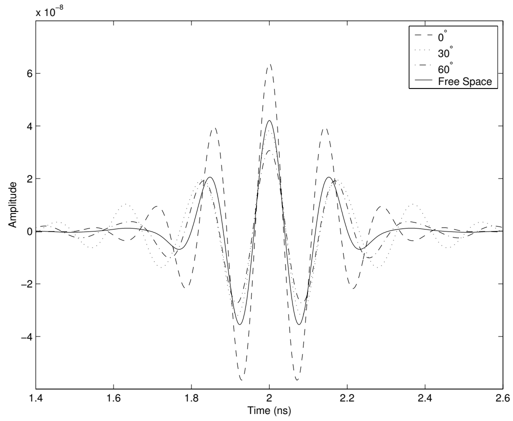

Fig. 9. Output of matched filter: optimal.

shall be introduced. Even in the case, similar discussion can be done on the definition of the gain. To know the individual antenna parameters, three-antenna measurements shall be introduced.

This scheme is applicable for the evaluation of various UWB antennas. Therefore, some typical UWB antennas shall be evaluated by using the proposed technique.

Acknowledgement

The authors would like to thank Mr. Kimio Sakurai, Dr. Ichirou Ida, Mr. Gilbert S. Ching, Mr. Chulgyun Park, Mr. Katsuyuki Haneda, and Ms. Navarat Lertsirisopon, all in Tokyo Institute of Technology, for their helps in the experiments and reviewing the paper.

References

[1] J.D. Taylor, "Introduction to Ultra-Wideband Radar Systems," CRC press, London, UK, pp. 670, 1995.

[2] OSD/DARPA, "Ultra-Wideband Radar Review Panel," Assessment of Ultra-Wideband (UWB) Technology. Arlington, VA.: DARPA, 1990.

[3] K. Siwiak, "Ultra-Wide Radio: Introduccing a

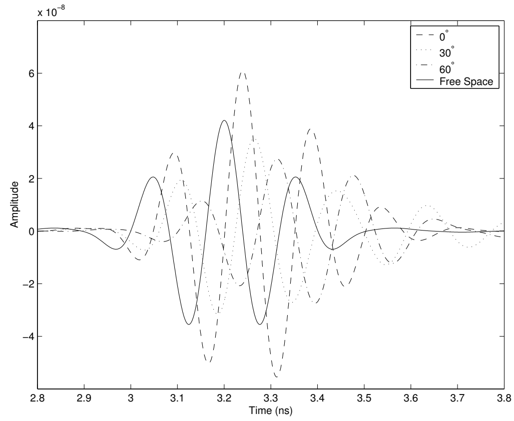

Fig. 10. Output of the matched filter: free space approximation.

Table 2. Relative gain of (antennas + matched filter), with respect to the ideal isotropic antennas.

Filter	Gain [dBi]		
	0°	30°	60°
Optimum	3.6	−0.8	−2.7
Isotropic approximation	3.2	−1.6	−3.7

Table 3. Correlation coefficient between the impulse responses of the received signal and the approximate matched filter by using isotropic antennas.

Orientation	0°	30°	60°
Correlation	0.96	0.91	0.86

New Technology," *2001 Spring IEEE Veh. Tech. Conf. (VTC)*, Plenary session, May 2001.

[4] K. Siwiak, "Ultra-Wide Radio: The emergence of an Important RF Technology", *Proc. 2001 Spring IEEE Veh. Tech. Conf. (VTC)*, May 2001.

[5] J. Farserotu, A. Hutter, F. Platbrood, J. Gerrits, A. Pollini, "UWB Transmission and MIMO Antenna Systems for Nomadic User and Mobile PAN," *Wireless Personal Commun.*, no. 22, pp. 197–317, 2002.

[6] Federal Communications Commission, "Revision of Part 15 of the Commission's Rules Regarding Ultra-Wideband Transmission Systems," First Report and Order, FCC 02–48, Apr. 2002.

[7] K. Siwiak, "Impact of UWB Transmission on Generic Receiver," *Proc. IEEE Veh. Tech. Conf. (VTC)*, May 2001.

[8] H. Schantz, "Measurement of UWB Antenna Efficiency," *Proc. IEEE Veh. Tech. Conf. (VTC)*, May 2001.

[9] H.F. Harmuth and S. Ding-Rong, "Antennas for Nonsinusiodal Wave — Part I: Radiators," *IEEE Trans. Elec. Mag. Compat.*, vol. EMC–25, no. 1,

pp. 13–24, Feb. 1983.
[10] H.F. Harmuth and S. Ding-Rong, "Antennas for Nonsinusiodal Wave — Part II: Sensors," *IEEE Trans. on Elec. Mag. Compat.*, vol. EMC–25, no. 1, no. 2, pp. 107–115, May 1983.
[11] H.T. Friis, "A Note on a Simple Transmission Formula," *Proc. IRE*, vol. 34, no. 5, pp. 254–256, May 1946.
[12] J. Takada, S. Promwong and W. Hachitani, "Extension of Friis' Transmission Formula for Ultra Wideband Systems," *IEICE Tech. Rep.*, WBS2003-*/MW2003-*, May 2003.
[13] S. Promwong, W. Hachitani,and J. Takada, "Experimental Study of Ultra-Wideband Transmission Based on Friis' Transmission Formula," *ISCIT2003-**, Songkhla, Thailand, SEPT 2003.
[14] M. K. Y. Lai, A.L. Sinopoli and W.D. Burnside, "A Novel Antennas for Ultra-Wideband Applications," *IEEE Trans. Antennas Propagat.*, vol. AP-40, no. 7, pp. 755–760, July 1992.

Sathaporn Promwong received the B.E. degree in Electronics Engineering and M.E. degree in Electrical Engineering from King Mongkut's Institute of Technology Ladkrabang, Bangkok, Thailand, in 1994 and 1999, respectively. He is currently working toward the Ph.D. degree in Tokyo Institute of Technology, Tokyo, Japan.

Since 1995, he has joined in the department of Information Engineering, Faculty of Engineering, King Mongkut's Institute of Technology Ladkrabang. His research is interested in the area of Ultra Wideband (UWB) communications and antenna propagation. He is presently a member of the IEICE and IEEE.

Wataru Hachitani, photograph and biography not available at time of publication.

Jun-ichi Takada was born in Tokyo, Japan in 1964. He received the B.E., M.E. and D.E. degrees from Tokyo Institute of Technology, Japan, in 1987, 1989 and 1992, respectively. From 1992 to 1994, he has been a Research Associate at Chiba University, Chiba, Japan. From 1994, he has been an Associate Professor at Tokyo Institute of Technology, Tokyo, Japan. His current interested are mobile propagation and channel modeling, array signal processing and numerical simulation of waves.

Dr. Takada received the Excellent Paper Award and Young Engineer Award from IEICE, Japan in 1993 and 1994, respectively. He is a member of the IEICE, ACES, SIAM and AGU.

Pichaya Supanakoon received the B.E. degree in Telecommunication Engineering and M.E. degree in Electrical Engineering both from King Mongkut's Institute of Technology Ladkrabang, Bangkok, Thailand, in 1998 and 2000, respectively.

Since 1999, he has been with the Department of Information Engineering, Faculty of Engineering, King Mongkut's Institute of Technology Ladkrabang, as Lecturer. His research interests are in electromagnetic field computation, finite-difference time-domain (FDTD) method, electromagnetic compatibility, and radio wave propagation.

Monchai Chamchoy received the B.E. (with honors) degree in Electronics Engineering and M.E. degree in Electrical Engineering both from King Mongkut's Institute of Technology Ladkrabang, Bangkok, Thailand, in 1996 and 2000, respectively.

Since 1997, he was a Faculty Member at King Mongkut's Institute of Technology Ladkrabang. His main research interests are microwave and RF circuits design, array signal processing, and wireless communications. He is a member of the Institute of Electrical and Electronics Engineers (IEEE).

Prakit Tangtisanon, photograph and biography not available at time of publication.

Vech Vivek, photograph and biography not available at time of publication.